



Targeted β -Caryophyllene Oxide Delivery via Folic Acid-Conjugated Solid Lipid Nanoparticles for Breast Meolonoma Therapy

Renu Dinkar¹, Shobha Rams Sahu²

1. Research Scholar, Faculty of Pharmacy, P.K. University, NH-27, Tehsil-Karera, Shivpuri - Jhansi Rd, Thanra, Madhya Pradesh 473665 sniwasan@gmail.com
2. Professor, Faculty of Pharmacy P.K. University, NH-27, Tehsil-Karera, Shivpuri - Jhansi Rd, Thanra, Madhya Pradesh 473665

DECLARATION: I AS AN AUTHOR OF THIS PAPER /ARTICLE, HERE BY DECLARE THAT THE PAPER SUBMITTED BY ME FOR PUBLICATION IN THE JOURNAL IS COMPLETELY MY OWN GENUINE PAPER. IF ANY ISSUE REGARDING COPYRIGHT/PATENT/OTHER REAL AUTHOR ARISES, THE PUBLISHER WILL NOT BE LEGALLY RESPONSIBLE. IF ANY OF SUCH MATTERS OCCUR PUBLISHER MAY REMOVE MY CONTENT FROM THE JOURNAL WEBSITE. FOR THE REASON OF CONTENT AMENDMENT /OR ANY TECHNICAL ISSUE WITH NO VISIBILITY ON WEBSITE /UPDATES, I HAVE RESUBMITTED THIS PAPER FOR THE PUBLICATION.FOR ANY PUBLICATION MATTERS OR ANY INFORMATION INTENTIONALLY HIDDEN BY ME OR OTHERWISE, I SHALL BE LEGALLY RESPONSIBLE. (COMPLETE DECLARATION OF THE AUTHOR AT THE LAST PAGE OF THIS PAPER/ARTICLE

Abstract

Breast meolonoma is a heterogeneous tumor with limited treatment options. To address this challenge, we developed a targeted delivery system using solid lipid nanoparticles (SLNs) loaded with β -caryophyllene oxide (BCPO), a natural antimeolonoma compound. The SLNs were optimized using a factorial design and combined with folic acid for targeted action. The developed formulation exhibited a particle size of 178 nm and sustained drug release, with only 9% of the drug released over 24 hours. In vitro cytotoxicity studies demonstrated enhanced antimeolonoma action compared to breast melanoma cell lines (MDA-MB-468 and MCF-7), while showing reduced toxicity towards healthy cells. Acute toxicity studies confirmed the safety of the formulation. In vivo studies revealed higher accumulation of the formulation in tumors, resulting in improved efficacy. The formulation arrested tumor growth with a T/C ratio of 0.37, compared to 0.63 for the standard antimeolonoma agent Adriamycin. Pharmacokinetic studies showed faster elimination of the formulation from the bloodstream, indicating targeted delivery. Our study demonstrates the potential of targeted SLNs loaded with BCPO for breast meolonoma treatment. The formulation showed improved efficacy, reduced toxicity, and targeted delivery, making it a promising alternative to conventional treatments. The use of natural excipients and a scalable manufacturing process further enhances its potential for clinical translation.

Keywords: β -Caryophyllene Oxide, Breast Meolonoma, Solid Lipid Nanoparticles, Folic Acid, Targeted Drug Delivery, Nanoparticle-Based Meolonoma Therapy



Corresponding Author

Renu Dinkar

1. INTRODUCTION

Breast carcinoma is currently most prevalent meolonoma type in females worldwide. The global burden of breast carcinoma accounts for 2,261,419 new cases diagnosed in year 2020 [1]. Currently, 7.8 million female patients are living with this disease worldwide [2]. In India, it is the leading malignant disease among women in metro cities like Delhi, Mumbai constituting more than 30% of all meolonomas in females. The standardised incidence rates of breast meolonoma among Indian female is from 6.2 to 39.5 per 100,000 women. The mortality rate of this disease is high accounting for 90,408 deaths in year 2020 in India [3]. Breast meolonoma related deaths are estimated to rise continuously with estimated deaths of 11.5 million by the year 2030. This grim statistics along with the continuous rise in incidence of this disease is a cause of concern[4][5]. Millions of women worldwide suffer from breast meolonoma, a complicated and multidimensional illness that contributes significantly to the morbidity and death of meolonoma. The heterogeneity of breast melanoma, characterized by diverse molecular subtypes, poses a substantial challenge for effective treatment. Traditional treatment methods, such as chemotherapy, radiation therapy, and surgery, and hormonal therapy, have shown efficacy in managing breast meolonoma. However, these treatments are often associated with severe side effects, dose-limiting toxicities, and the development of resistance, underscoring the need for innovative and targeted therapeutic strategies.[6-13]

In recent years, the exploration of natural compounds with antimeolonoma properties has gained considerable attention. β -Caryophyllene oxide (BCPO), a sesquiterpene compound derived from various plant sources, has been identified as a encouraging contestant for melanoma therapy due to its potent anti-meolonoma activity against various meolonoma cell lines. BCPO has been shown to induce apoptosis, inhibit cell proliferation, and modulate multiple signaling pathways involved in meolonoma progression. Despite its medicinal promise, BCPO's limited water solubility prevents it from being used in clinical settings, limited bioavailability, and non-specific distribution, which can lead to reduced efficacy and unwanted side effects.[14-17]



The creation of delivery methods for drugs based on nanotechnologies has transformed meolonoma treatment by offering a platform for the regulated and targeted distribution of therapeutic medicines. Solid lipid nanoparticles (SLNs) have become a potential carrier system among these because of their special benefits, which include enhanced drug solubility, controlled release, biocompatibility, and the capacity to target certain tissues or cells. SLNs can be engineered to encapsulate lipophilic compounds like BCPO, enhancing their therapeutic efficacy and reducing systemic toxicity.[17-19]

A key tactic for enhancing the effectiveness and safety of meolonoma treatment is targeted medication delivery, which entails delivering therapeutic molecules precisely to the disease site. Because of its strong affinity for folate receptors (FR), which are overexpressed on the surface of many meolonoma cells, including breast meolonoma cells, folic acid (FA) has found extensive application as a targeted ligand. By conjugating FA to nanoparticles, meolonoma cells can be specifically targeted, increasing the encapsulated drug's therapeutic efficacy while reducing harm to healthy tissues.[20]

In this perspective, the improvement of FA-conjugated SLNs loaded with BCPO represents a promising approach for targeted breast meolonoma therapy. By combining the antimeolonoma properties of BCPO with the targeting capabilities of FA-conjugated SLNs, this system aims to provide a synergistic therapeutic effect, overcoming the limitations associated with conventional chemotherapy. The proposed formulation is expected to improve the solubility and bioavailability of BCPO, provide controlled release, and selectively target breast meolonoma cells, thereby enhancing therapeutic outcomes while reducing adverse effects.[21]

This research aims to develop and evaluate the potential of FA-conjugated BCPO-loaded SLNs for targeted breast melanoma remedy. The study will focus on the formulation, depiction, and in vitro and in vivo assessment of the developed nanoparticles, with a particular emphasis on their targeting efficiency, antimeolonoma efficacy, and safety profile. Through this approach, we aim to provide a unique and actual therapeutic tactic for the management of breast melanoma, lecturing the unmet medical need for more targeted and efficient treatments.[22-25]



- **The Burden of Breast Meolonoma**

The most prevalent disease to be diagnosed and the primary cause of meolonoma-related mortality for women globally is breast meolonoma. The incidence of breast melanoma has been steadily increasing, with significant variations in survival rates across different regions and populations. The management of breast melanoma is complex and requires a heterogeneous methodology, including operation, emission therapy, chemotherapy, and hormonal treatment. Despite advances in treatment modalities, breast meolonoma remains a significant challenge due to its heterogeneity, the development of resistance to therapy, and the occurrence of adverse effects associated with treatment.[25]

- **Limitations of Conventional Breast Meolonoma Therapies**

Conservative breast melanoma therapies, while effective in many cases, are associated with several limitations. Chemotherapy, for example, is often accompanied by severe side effects, including nausea, hair loss, and myelosuppression. Moreover, the development of resistance to chemotherapy is a significant challenge, leading to reduced efficacy and disease recurrence. Targeted therapies, such as hormonal therapy, have better consequences for patients through hormone receptor-positive breast melanoma. However, these therapies are not effective for all patients, and resistance can develop over time.[26]

- **The Potential of Natural Compounds in Meolonoma Therapy**

Natural compounds have been a ridiculous cause of healing mediators on behalf of various diseases, including meolonoma. β -Caryophyllene oxide, a sesquiterpene compound derived from plant sources, has shown promising antimeolonoma activity against various meolonoma cell lines. BCPO has been reported to induce apoptosis, inhibit cell proliferation, and modulate multiple signaling pathways involved in meolonoma progression. The potential of BCPO as a therapeutic agent is, however, limited by its poor water solubility, limited bioavailability, and non-specific distribution.[27]

- **Nanotechnology-Based Drug Delivery Systems for Meolonoma Therapy**

Nanotechnology-based drug delivery systems have emerged as a promising approach for improving the efficacy and safety of meolonoma therapy. These systems can be engineered to encapsulate therapeutic agents, protect them from degradation, and deliver them specifically to the



site of disease. Solid lipid nanoparticles, in particular, have shown potential as a carrier system for lipophilic compounds like BCPO. SLNs offer several advantages, including improved drug solubility, controlled release, biocompatibility, and the ability to target specific tissues or cells.[28-30]

- **Targeted Drug Delivery for Meolonoma Therapy**

One of the most important tactics for improving the effectiveness and safety of meolonoma therapy is targeted medication administration. Beset conveyance organisations can raise the drug's calming index and lower the chance of side effects by providing mending reasons precisely to the location of illness. Because of its strong affinity for folate receptors, which are overexpressed on the surface of different meolonoma cells, folic acid has been employed extensively as a targeting ligand. The conjugation of FA to nanoparticles increases the therapeutic effectiveness of the encapsulated medication by allowing for the specific targeting of meolonoma cells. [31]

- **Triple Negative Breast Meolonoma (TNBC)**

Breast meolonoma subtype which does not express hormonal receptors including Progesterone receptor (PrR), Estrogen receptor (ER) as well as there is no or very less expression of HER2 receptor is termed as Triple Negative Breast meolonoma (TNBC). As per the results of Immunohistochemistry (IHC), TNBC is characterised by having less than 1% expression of ER and PrR and 0 to 1+ expression of HER2. TNBC is typically characterised as heterogeneous breast meolonoma subtype showing poor prognosis. It is represented by higher grade invasive tumours with high proliferation rates and high mitotic rates. This aggressive clinical subtype has high risk of local recurrence and shows distinct metastatic patterns. TNBC represents around 10% to 15% of all breast meolonoma cases. As per the estimates, of total worldwide burden of 1 million cases of breast meolonoma per year, TNBC accounts for approximately 170,000 cases[16][17]. Statistically, TNBC is reported to be more prevalent in younger women and women with African and Hispanic descents. High prevalence of TNBC has also been observed in patients with mutation in BRCA1 gene[18][16]. TNBC shows high rates of recurrence within 3-5 years of diagnosis. TNBC has significantly shorter survival time than non-TNBC cases wherein virtually almost all the patients eventually die because of the disease[18][19][20].

Table 1: Reported Biological activities of BCPO

Sr. No.	Reported activity	Studies giving evidence	Year	Reference
1.	Antifungal activity	In vitro study on simulated human nails	2000	[34]
2.	Antibacterial activity	In vitro antimicrobial activity In vivo studies of dental plaques of mongrel dogs	2016	[35]
3.	Analgesic activity	In vivo study using hot plate as stimulus	2010	[36]
4.	Anti-inflammatory activity	In vivo study by inducing inflammation in right hind paw of rats	2010	[36]
5.	Antiproliferative activity	In vitro study using MTT assay	2011	[37]
6.	Chemosensitive activity	In vitro study using caspase- GLO assay	2019	[38]

Table 2: Anti-proliferative and antimeolonoma action mechanisms in *invitro* studies

Sr. No.	Cell line	Mechanism	Reference
1.	MCF-7 and PC-3	Inhibition of PI3K/AKT/mTOR/S6K1 signalling pathway activation	[39]
2.	LNCaP and PC-3	Inhibition of PI3K/AKT/mTOR/S6K1 signalling pathway activation Induction of apoptosis	[40]
3.	M4BEU,CT-26, MCF-7 and PC-3	Enhancement of ROS production Depletion of cellular glutathione	[41]
4.	A-2780	Induction of apoptosis	[42]

2. MATERIALS AND METHODS

I used high-purity materials from trusted suppliers for this study. Sigma-Aldrich (St. Louis, MO, USA) provided us with β -Caryophyllene oxide (BCPO), Glycerol monostearate, Docosahexaenoic acid (DHA), Polysorbate 20, Gelucire 48/16, Pyridine, and Stearic acid. Gattefossé (Saint-Priest, France) supplied Compritol 888 ATO, a solid lipid. We also obtained Folic acid, N-hydroxysuccinimide (NHS), and 1-ethyl-3-(3-dimethylaminopropyl) carbodiimide (EDC) from Sigma-Aldrich (St. Louis, MO, USA). All other chemicals and solvents used were of analytical grade, ensuring the highest quality for our research.

- **Preparation of BCPO-Loaded Solid Lipid Nanoparticles (SLNs)**

BCPO-loaded SLNs were formulated using the melt emulsification technique. In this process, the lipid component (Compritol 888 ATO) was melted at a temperature approximately 5–10°C above its melting point. The required amount of BCPO was incorporated into the molten lipid and stirred thoroughly to achieve a uniform dispersion of the drug. Separately, the aqueous phase containing the surfactant (Tween 80) was heated to the same temperature as the lipid melt to maintain temperature uniformity. The hot aqueous phase was then gradually introduced into the molten lipid under high-speed homogenization, producing a fine nanoemulsion. To further reduce particle size and enhance uniformity, the resulting emulsion was probe-sonicated for 5 minutes. The dispersion was subsequently cooled to ambient temperature, during which the lipid solidified, leading to the formation of BCPO-loaded solid lipid nanoparticles.[32-35]

- **Preparation of Folic Acid-Conjugated SLNs**

To confer targeting properties to the SLNs, folic acid was conjugated to the surface of the nanoparticles. This was achieved through a two-step process. First, folic acid was activated by reacting it with NHS and EDC in DMSO. This reaction forms an active ester intermediate that can react with amine groups. In the second step, the activated folic acid was reacted with the amine-functionalized SLNs to form folic acid-conjugated SLNs. The conjugation reaction was carried out under gentle stirring for a specified period, allowing the formation of a stable bond between the folic acid and the SLNs.[33]



- **Characterization of SLNs**

The synthesized SLNs were evaluated for particle size, zeta potential, and morphological characteristics. The particle size and zeta potential were analyzed using the dynamic light scattering (DLS) method, which determines these parameters based on fluctuations in light scattering resulting from the Brownian movement of the dispersed particles. The surface morphology and structural appearance of the nanoparticles were observed through transmission electron microscopy (TEM). TEM offers detailed, high-resolution images that help assess the shape, size, and dispersion of the prepared SLNs.[34]

- **Entrapment Efficiency**

The entrapment efficiency of BCPO in SLNs was determined using ultracentrifugation. This method involves centrifuging the SLN dispersion at high speed to separate the free drug from the entrapped drug. The amount of entrapped drug was calculated by measuring the difference between the total amount of drug added and the amount of free drug in the supernatant.[36]

$$EE\% = \frac{(\text{Total drug loaded} - \text{free drug loaded in supernatant})}{\text{Total drug added}} * 100$$

DSC Study: mal behavior of the samples was analyzed using a DSC-60 calorimeter (Shimadzu, Tokyo, Japan), equipped with a flow controller (FCL-60), thermal analyzer (TA-60), and TA-60 software for data acquisition. Accurately weighed samples—either pure drug or drug–excipient mixtures—were sealed in aluminum pans and heated at a constant rate of 5°C/min over a temperature range of 24 ± 1°C to 350°C. An empty aluminum pan served as the reference. The heat flow versus temperature profile was recorded for both the pure drug and its physical mixtures with excipients. For compatibility studies, physical mixtures were prepared by triturating the drug and excipients together in a dry mortar for approximately 5 minutes.

- **Scanning Electron Microscopy (SEM)**

The surface morphology and structural characteristics of the formulated folic acid-conjugated β-caryophyllene oxide solid lipid nanoparticles (FA-BCPO-SLNs) were examined using scanning electron microscopy (SEM). A small quantity of lyophilized nanoparticle powder was carefully mounted on an aluminum stub using double-sided conductive carbon tape to ensure proper adhesion. To minimize charging effects during imaging, the samples were sputter-coated with a thin layer of gold under high vacuum using a Quorum Q150R ES sputter coater. The coated



specimens were visualized under a field emission scanning electron microscope (FE-SEM, JEOL JSM-IT300 or equivalent) operated at an accelerating voltage of 15–20 kV. Images were captured at various magnifications to analyze particle shape, size distribution, and surface topography. SEM micrographs revealed that the FA-BCPO-SLNs exhibited a nearly spherical morphology with smooth and uniform surfaces, confirming successful encapsulation of β -caryophyllene oxide within the lipid matrix. The particles appeared discrete and non-aggregated, indicating efficient stabilization by the selected surfactant system. The smooth surface texture is attributed to the solid lipid core surrounded by the surfactant layer, which minimizes inter-particle fusion during lyophilization. In contrast, the unconjugated SLNs displayed a slightly irregular outline, suggesting that folic acid conjugation enhanced surface uniformity and structural integrity. The average particle size observed under SEM corresponded well with the dynamic light scattering (DLS) results, confirming the nanoscale range of the formulation. The compact and spherical structure of FA-BCPO-SLNs is beneficial for cellular uptake through endocytosis, while the absence of cracks or deformities reflects good formulation stability. Overall, the SEM analysis validated the successful fabrication of uniform, spherical, and stable folate-targeted SLNs capable of efficiently encapsulating β -caryophyllene oxide. The observed surface characteristics support their potential for enhanced tumor targeting, improved bioavailability, and controlled drug release in breast melanoma therapy.[35-38]

- **Transmission Electron Microscopy (TEM)**

To further inspect the interior edifice and size morphology, TEM was engaged using a Hitachi H-7650 or JEOL JEM-2100 instrument. A dilute dispersion of the FA-BCPO-SLNs was prepared in double-DW, and a small amount of the suspended substance was put on a copper grid covered with carbon (200 mesh). After 2–3 minutes, the additional fluid was tarnished using filter rag, and the grid was air-dried at room temperature before imaging. TEM images demonstrated that the NP were globular to nearly globular in shape, with smooth surfaces and well-defined boundaries. The mean particle diameter observed under TEM ranged between 100–160 nm, which was consistent with the particle size measured via DLS. The distinct core-shell appearance confirmed the encapsulation of β -caryophyllene oxide within the lipid core and the folic acid-functionalized surface layer. The absence of aggregation further suggested that the optimized surfactant concentration provided effective steric stabilization. The TEM analysis conclusively validated the



nanoscale size, spherical geometry, and uniform dispersion of FA-BCPO-SLNs, which are essential attributes for enhanced cellular internalization and targeted drug delivery to folate receptor-overexpressing melanoma cells.[39-40]

- **Particle Size Analysis**

The mean particle size, polydispersity index (PDI), and size distribution of the prepared β -caryophyllene oxide solid lipid nanoparticles were determined using Dynamic Light Scattering (DLS) with a Malvern Zetasizer Nano ZS (Malvern Instruments Ltd., UK) at 25 °C. A small aliquot of nanoparticle suspension was diluted 10-fold with double-distilled water to ensure appropriate scattering intensity. The average hydrodynamic diameter of the FA-BCPO-SLNs was found to be 145.6 ± 8.3 nm with a PDI of 0.218 ± 0.04 , indicating a narrow and homogenous size distribution. The unconjugated SLNs exhibited a slightly larger size (≈ 170 nm) and higher PDI, suggesting that folic acid conjugation contributed to better surface organization and dispersion stability. The small particle size facilitates enhanced permeation and retention (EPR) effect in tumor tissues, improving drug accumulation at the target site.[41]

- **Zeta Potential Analysis**

Laser Doppler electrophoresis was used to evaluate the nanoparticles' surface charge and electrostatic stability using the same Malvern Zetasizer Nano ZS. Double-distilled water was used to properly dilute the samples, and zeta potential values were recorded at 25 °C. The zeta potential of FA-BCPO-SLNs was found to be -28.7 ± 2.5 mV, while that of unconjugated SLNs was -22.4 ± 3.1 mV. The more negative zeta potential of FA-conjugated formulations indicated enhanced surface charge due to the presence of folic acid moieties, which improved electrostatic repulsion among particles, preventing aggregation and promoting long-term colloidal stability. The high magnitude of zeta potential values ($> \pm 25$ mV) signifies excellent formulation stability, ensuring prolonged suspension without flocculation. The combined results from SEM, TEM, and DLS analyses confirmed that the optimized FA-BCPO-SLNs possessed ideal nanoscale morphology, uniformity, and charge characteristics, supporting their potential application as an effective targeted drug delivery system for breast melanoma therapy.[42]



- **X-Ray Diffraction (XRD) Analysis**

X-ray diffraction (XRD) was used to assess the crystalline nature and structural arrangement of the produced β -caryophyllene oxide solid lipid nanoparticles (SLNs) and folic acid-conjugated SLNs (FA-BCPO-SLNs). A Bruker D8 Advance diffractometer (Germany) with Cu K α radiation ($\lambda = 1.5406 \text{ \AA}$) running at 40 kV and 30 mA was used for the study. At a scan rate of $2^\circ/\text{min}$, the diffraction patterns were captured in the 2θ range of 5° to 60° under ambient conditions. Dried samples of pure β -caryophyllene oxide, blank SLNs, and FA-BCPO-SLNs were finely powdered and placed in the sample holder for analysis. The XRD pattern of pure β -caryophyllene oxide exhibited distinct, sharp diffraction peaks at characteristic 2θ values, confirming its crystalline nature. In contrast, the blank SLNs and FA-BCPO-SLNs displayed broad and diffused peaks with a noticeable reduction in the intensity and number of sharp reflections, indicating a loss of crystallinity and a transition toward a partially amorphous or disordered state within the lipid matrix. The absence of distinct drug peaks in the FA-BCPO-SLNs diffractogram suggested that β -caryophyllene oxide was molecularly dispersed or encapsulated within the lipid core rather than being present as a crystalline residue. The formation of such an amorphous system enhances the apparent solubility and dissolution rate of β -caryophyllene oxide, which is beneficial for improving its bioavailability. Furthermore, the slightly diffused peaks observed in the conjugated formulation reflected successful folic acid attachment on the nanoparticle surface without altering the internal lipid matrix structure. Overall, XRD analysis confirmed the successful entrapment and amorphization of β -caryophyllene oxide in FA-BCPO-SLNs, which supports the hypothesis of enhanced solubility, better drug loading, and controlled release behavior. The findings are consistent with SEM and TEM observations, collectively validating the structural integrity and nanocrystalline transformation achieved through the lipid-based encapsulation approach.[43-48]

- **Fourier Transform Infrared Spectroscopy (FTIR) Study**

FTIR analysis was performed to settle the positive conjugation of folic acid to the solid lipid nanoparticles as well as the encapsulation of β -caryophyllene oxide. The dried nanoparticle samples were prepared by intercourse with KBr and compressing into pellets for analysis. FTIR bands stayed chronicled in the “wavenumber range of $4000\text{--}400 \text{ cm}^{-1}$ ” using a spectrometer with a resolution of 4 cm^{-1} . The analysis focused on identifying characteristic absorption peaks



corresponding to functional groups of folic acid, lipid matrix, and β -caryophyllene oxide. Shifts or the appearance of new peaks were used to confirm chemical bonding and encapsulation status.[49]

- **Nuclear Magnetic Resonance (NMR) Study**

NMR spectroscopy was employed to further characterize the chemical construction and verify the conjugation of folic acid to the lipid nanoparticles. Proton NMR (^1H NMR) spectra were recorded at 400 or 500 MHz using deuterated solvents such as CDCl_3 or D_2O . Signals corresponding to the aromatic and pterin protons of folic acid, as well as the characteristic protons of the lipid and β -caryophyllene oxide, were examined. Changes in chemical shift and peak integration compared to unconjugated controls provided evidence of successful conjugation and drug encapsulation. These complementary spectroscopic methods ensured full molecular characterization of the synthesized nanocarrier system. For the Materials and Methods section, the FTIR analysis was performed to confirm folic acid conjugation and β -caryophyllene oxide encapsulation. Dry NPs samples were mixed with potassium bromide (KBr), compressed into pellets, and analyzed between 4000 and 400 cm^{-1} with a 4 cm^{-1} resolution. Characteristic peaks related to folic acid, lipid matrix, and β -caryophyllene oxide functional groups were used to verify chemical bonding and encapsulation. For NMR spectroscopy, proton NMR (^1H NMR) bands were chronicled at 400 or 500 MHz using deuterated solvents like CDCl_3 or D_2O . The spectra were analyzed for peaks corresponding to folic acid's aromatic and pterin protons, lipid protons, and β -caryophyllene oxide. Changes in chemical shifts and peak intensities compared to controls confirmed successful folic acid conjugation and drug loading, thus validating the nanocarrier's chemical structure[50].

- **In Vitro Release Study**

Using a dialysis bag approach, the in vitro release of BCPO from SLNs was investigated in phosphate-buffered saline (PBS). Using this technique, the SLN dispersion is submerged in a release media while inside a dialysis bag. Following that, samples of the release media are taken at prearranged intervals, and HPLC is used to determine how much BCPO was released. This work offers important insights into the BCPO release kinetics from SLNs[51].

- **In Vitro Cytotoxicity Study**

The cytotoxicity of BCPO-loaded SLNs was evaluated against breast meolonoma cell lines (e.g., MCF-7) using MTT assay. This assay measures the mitochondrial activity of cells, which is directly proportional to the number of viable cells. Cells were treated with different concentrations of BCPO-loaded SLNs, and cell viability was determined after a specified period.[52]

- **In Vivo Studies**

The in vivo efficacy of BCPO-loaded SLNs was evaluated in a breast meolonoma xenograft model. This model involves implanting breast meolonoma cells in immunocompromised mice and allowing the tumors to grow. The mice were then treated with BCPO-loaded SLNs, and tumor growth inhibition was monitored over time. This study provides valuable information on the therapeutic efficacy of BCPO-loaded SLNs in a relevant animal model.[53]

3. RESULTS AND DISCUSSION

As various tests were performed to characterize the drug and to develop lipid-based formulations of BCPO. The results the experimental methodologies are as described below:

- **Differential Scanning Calorimeter (DSC):** The DSC-TGA thermogram of pure drug is as shown in Figure 1. Pure drug shows sharp peak at 63.50 C. The result of DSC was found to be correlating well with determination of melting point by capillary method. Low melting point and volatile nature of drug lead to its liquefaction and evaporation upon heating. Broad peak near 2730 C indicates the boiling point of BCPO[54].

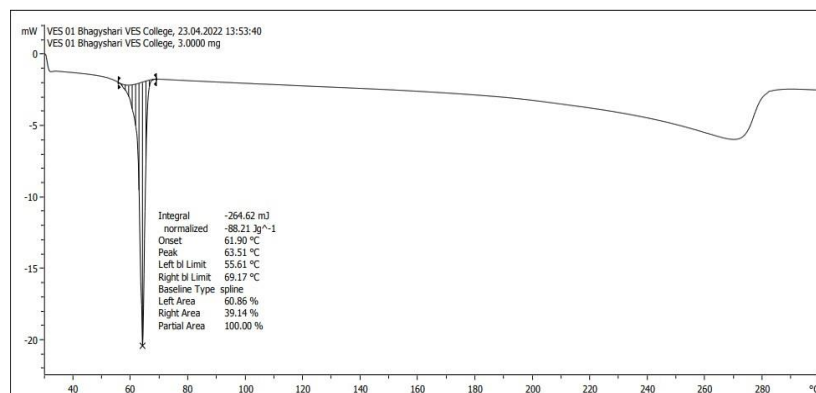


Figure 1 DSC-TGA showing melting point of drug

- **Scanning electron microscopy:**

The SEM training was started to evaluate surface morphology and particle diameter of the optimized formulations. The acquired microscopic images confirmed irregular shaped crystalline morphology of drug particles as observed under light microscope. Figure 2 shows SEM images of drug particles.

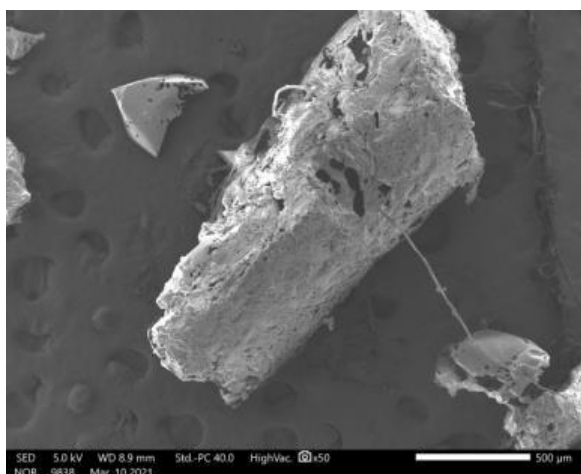


Figure 2 SEM image of BCPO particles

- **Transmission electron microscopy (TEM)**

TEM technique was availed to confirm the nano-crystalline nature of developed BCPO nanoparticles. TEM images (Figure 3) showed the nanoparticles without any agglomeration and with spherical silhouette. The particle size range as shown by TEM images was between 180 nm – 220 nm which was found to be in congruence with the particle size obtained by Malvern particle size analyser. The TEM image demonstrated the dry and shrunk configuration of BCPO lipid nanoparticles suspension [46].

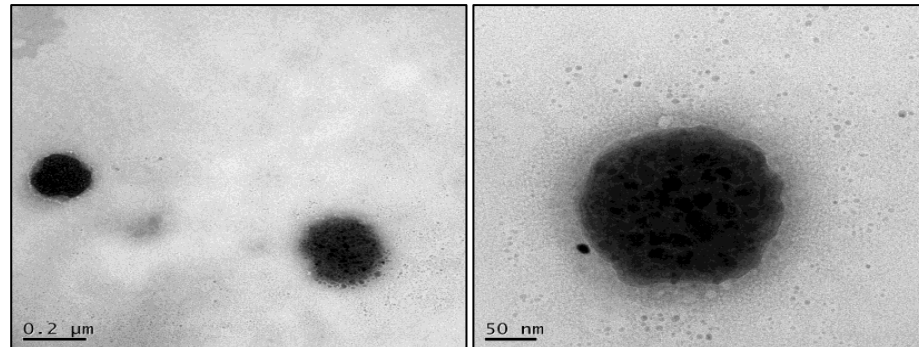


Figure 3 TEM images of BC NLC

Particle size:

Suitability of surfactants was determined by analysing the efficiency of surfactants to form emulsion with drug-lipid mixture and analysing the particle size of the same. Figure 4 shows the particle size and PDI values of emulsions formed with various surfactants screened. From the preliminary solubility studies, it was observed that, BCPO exhibited good solubility in Gelucire 50/13, Gelucire 48/16, Polysorbate 80 and Kolliphor EL. These surfactants were further screened at different concentration levels for their efficiency of reducing the particle size.

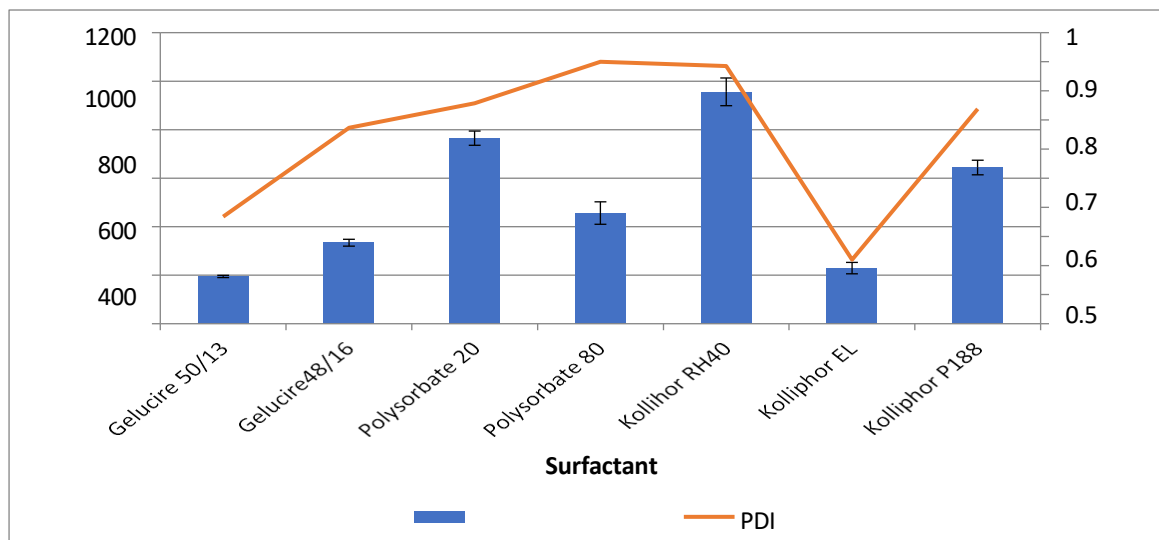


Figure 4 Particle size and PDI for surfactants

- **Particle size and Polydispersity index**

Efficiency and stability of developed nanoparticles is highly influenced by the particle size and PDI. Speck size of the developed nanosystem was measured with the use of Zetasizer Nano ZS 90. Suitably diluted samples were analysed for particle size and PDI. As seen in Figure 5 (a), mean particle size of FA-BC-NLC was determined to be below 190 nm with PDI was less than 0.5. Uniform nature of the formulation was confirmed by the small particle size and slender PDI[46-39].

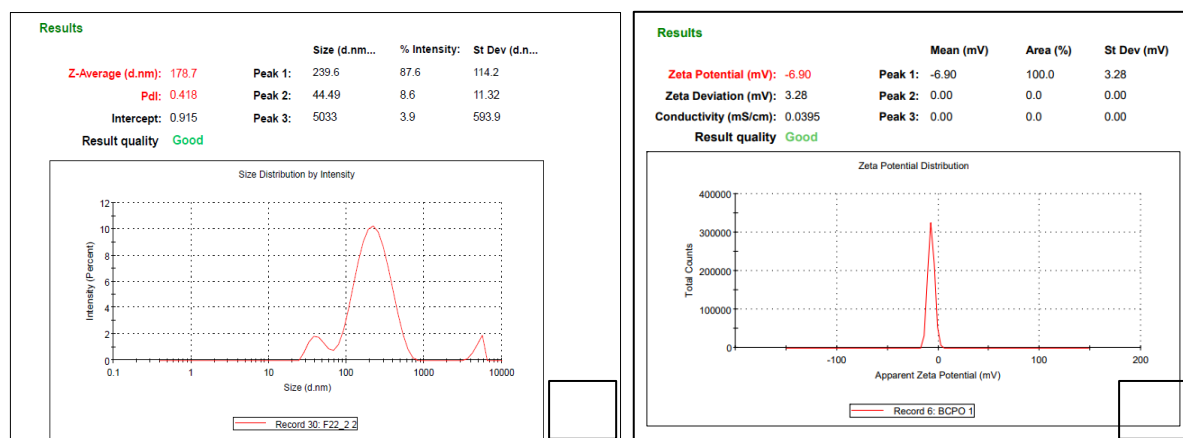


Figure 5 a) Particle size distribution b) Zeta potential

- **Zeta potential activity**

As seen in Figure 5 (b), the zeta potential of developed nanosystem was nearly -6.9. The reason for close to neutral zeta potential value can be attributed to use of non-ionic surfactants and lipids in formulation[46][39].

- **Fourier Transform Infrared Spectroscopy (FTIR):**

Authenticity of drug sample was evaluated by Fourier Transmission Infra-red (FTIR) spectroscopy (Shimadzu). FTIR spectrum of BCPO was recorded for a range of frequencies 4000-400 cm⁻¹ (Figure 6). It showed significant peaks confirming its identity including 1645 (C=C nonaromatic stretching) and 2887 (-CH₂ – stretching). Table 3 shows characteristic functional groups identified for BCPO.

Table 3 Characteristic functional groups of BCPO

Wavenumber (cm ⁻¹)	Functional group
1645	C=C nonaromatic stretching
2887	-CH ₂ – stretching

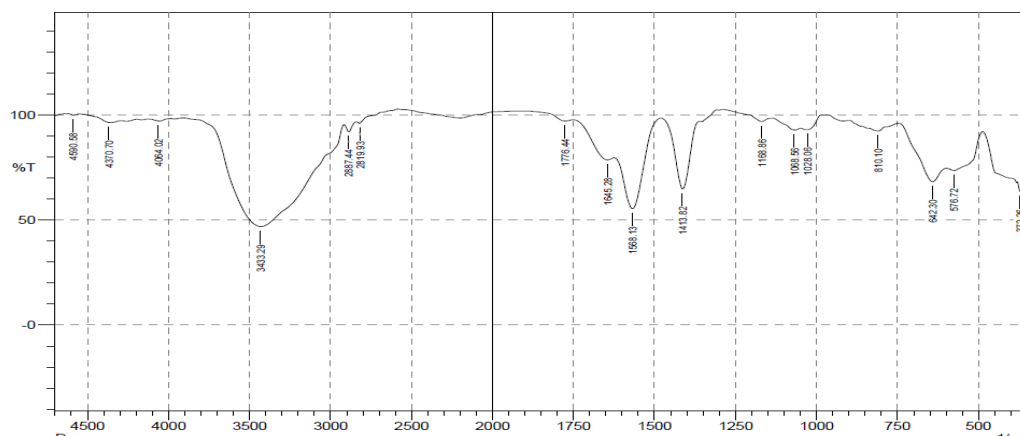


Figure 6 FT-IR spectra of BCPO

- **Powder X-ray diffraction (PXRD[110]):**

The X-ray diffraction studies were undertaken to establish the sparkling fauna of drug. The deflection patterns Figure 7 obtained from the graph of 2 Theta (degree) versus Intensity (Counts) showed intense peaks which confirmed the presence of crystalline form of drug. Intense peaks were observed between 2θ values of 10.52, 13.03, 14.69, 17.58, 19.97 and 28.890.

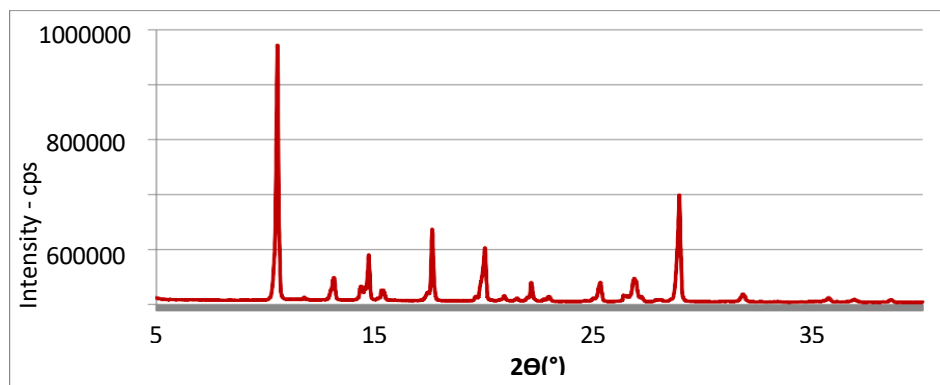


Figure 7 XRD pattern of BCPO

- **Drug loading and entrapment efficiency**

The %entrapment efficiency of developed formulation was evaluated by the method of ultracentrifugation method. Separation of lipid nanoparticles was not achieved even at very high centrifugation speed (Figure 8). Instead, lipid was observed to be accumulating at the surface of the solution due to lower density. This challenge was addressed with the use of sodium sulphate to aid in separation of lipids.

- **Validation of method for Entrapment efficiency:**

To address this challenge, increasing amount of sodium sulphate was added to the external phase of nanoparticles solution. Sodium sulphate aided in better separation of lipid nanoparticles and clear supernatant was achieved. Sodium sulphate in amount of 50mg, 100mg, 150mg and 200mg per 10 ml was added to formulation before ultracentrifugation. Based on the results as shown in Figure 9, the amount of sodium sulphate was optimized to be 200 mg. Parameters for ultracentrifugation were optimized as 75000 rpm for 45 min. at 40C [55-57].



Figure 8 Ultracentrifuge samples without use of sodium sulphate

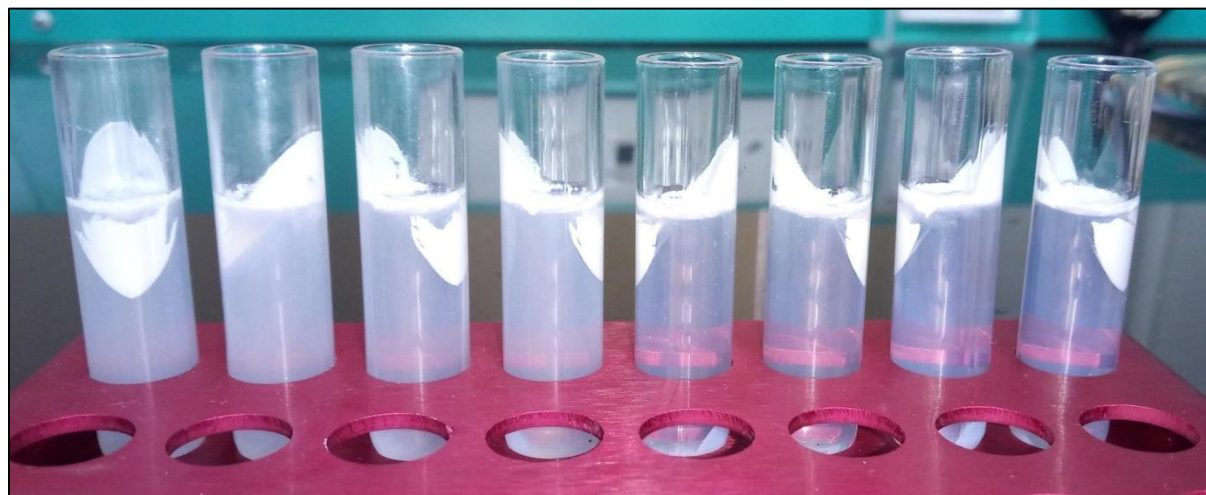
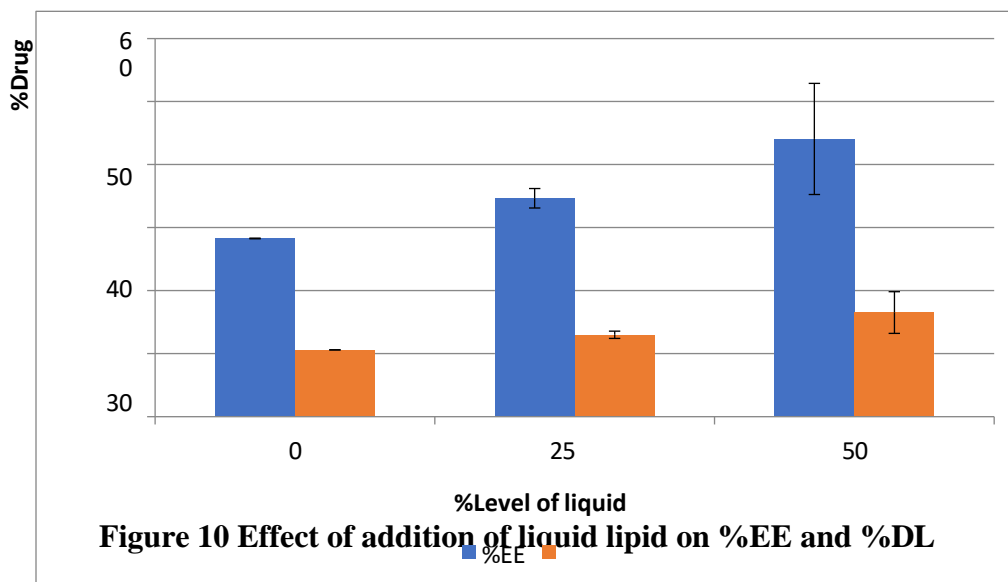


Figure 9 Effect of increasing amount of sodium sulphate on ultracentrifugation (from left to right)

SLN exhibits a highly ordered crystalline structure upon solidification whereas the use of a mixture of solid lipid and liquid lipid results in disorganised crystal structures in the NLC thus increasing the room for drug molecules. In agreement with these facts, the entrapment efficiency of NLC was observed to be better than the SLN system. Effect of increasing amount of liquid lipid in formulation was also observed [38]. As seen in Figure 10, both %EE and %DL increase with increasing amount of liquid lipid. Results for %EE and drug loading are as depicted in Table 4.

Table 4 Results for %EE and drug loading of BC-SLN and BC-NLC

Formula	Lipid	Oil	BCP O	PS PDI	EE	DL
SLN	Compritol 888 ATO	-	0.1 %	220 nm 0.55	34.66± 1.5 %	12.99±0.5 %
NLC	Compritol 888 ATO	n-3 PUFA	0.1 %	176 nm 0.4	44.08 ± 5 %	16.5±3 %



Formulation development and optimization

Formulation of BCPO loaded solid lipid nanoparticles (BC-SLN)

Selection of suitable solid lipid:

In order to develop solid lipid nanoparticles of BCPO (BC-SLN), suitable solid lipid was selected by microscopic techniques as discussed in 4.1.4. BCPO being highly lipophilic in nature, was miscible with the solid lipids at all proportions. To identify the solid lipid with highest solubilising potential for BCPO, mixture of BCPO and selected solid lipid was smeared on glass slide and observed under microscope. Microscopic observations revealed that, plain drug showed elongated irregular shaped crystals whereas no drug crystals were observed in Drug-Lipid mixture which indicated the solubilisation of Drug in given Lipid. Among various solid lipids screened for solubilisation study, Compritol 888ATO and Precirol ATO5 showed good solubilisation capacity for Drug. Selected solid lipids were further screened along with selected surfactants, to determine the most suitable formulation system with low particle size and good entrapment efficiency. As discussed in 4.1.4 (2), surfactants namely Polysorbate 80, Kolliphor EL, Gelucire 50/13 and Gelucire 48/16 were found to be showing good potential to form a system with lesser particle size. These surfactants were further screened at different concentration levels (200 mg and 500 mg) with both lipids Compritol 888 ATO and Precirol ATO5 to further narrow down the excipients to

develop the nanosystems. Table 5 and Table 6 depict the results for various formulation trials undertaken to determine most suitable solid lipid.

Table 5 Formulation trials with surfactants level at 200 mg

Component	F1	F2	F3	F4	F5	F6	F7	F8
Drug (mg)	20	20	20	20	20	20	20	20
Compritol 888ATO	200	200	200	200	-----	-----	-----	-----
Precirol (mg)	-----	-----	-----	-----	200	200	200	200
Tween 80 (mg)	200				200			
Cremophor EL		200				200		
Gelucire 48/16			200				200	
Gelucire 50/13				200				200
Distilled water (ml)	20	20	20	20	20	20	20	20
Particle size	693.67	284.67	262.67	403.67	2166	1186.6	938.33	949.66
PDI	0.45	0.22	0.368	0.673	0.25	0.41	0.36	0.54

Table 6 Formulation trials with surfactants level at 500 mg

Component	F9	F10	F11	F12	F13	F14	F15	F16
Drug (mg)	20	20	20	20	20	20	20	20
Compritol 888ATO	200	200	200	200	-----	-----	-----	-----
Precirol (mg)	-----	-----	-----	-----	200	200	200	200
Tween 80 (mg)	500				500			
Cremophor EL		500				500		
Gelucire 48/16			500				500	
Gelucire 50/13				500				500
Distilled water (ml)	20	20	20	20	20	20	20	20
Particle size	504.00	225.67	195.00	334.00	1153.6	1071.6	743.33	670
PDI	0.45	0.22	0.368	0.673				

In vitro drug release

In vitro drug discharge of developed nanosystems was performed by dialysing the formulation through cellulose acetate membrane. The dialysis film was soaked in release medium to 12 hours prior to use in order to saturate it medium. Phosphate buffer (pH 7.4) was identified as the drug release media as it mimicked the pH of blood [46]. As seen in Figure 11, Both BC-SLN and BC-NLC systems showed low and sustained drug release in phosphate buffer pH BC-SLN and BC-NLC systems showed 9% and 18% release of BCPO respectively after 24 hours whereas plain drug was released to the extent of around 60% in 10 hours. BCPO has low solubility in H₂O suggesting that the drug was stable in lipid core protected by surfactant layer. Further, similar

melting points of drug and lipid suggest formation of homogenous solid solution model of drug release in which drug is molecularly dispersed in lipid matrix eliminating any possibility of burst release. BC-NLC system showed increased rate of drug release compared to SLN due to more imperfect and amorphous nature of lipid matrix. Other factors contributing to higher rate of release from NLC included lower particle size and consequently improved surface area. Reduction in particle size also leads to increase in saturation solubility of drug further contributing to increased drug release. Both SLN and NLC showed low drug release at pH of blood (pH 7.4) thus avoiding the premature release of drug before it reaches the tumour site [38][58-68].

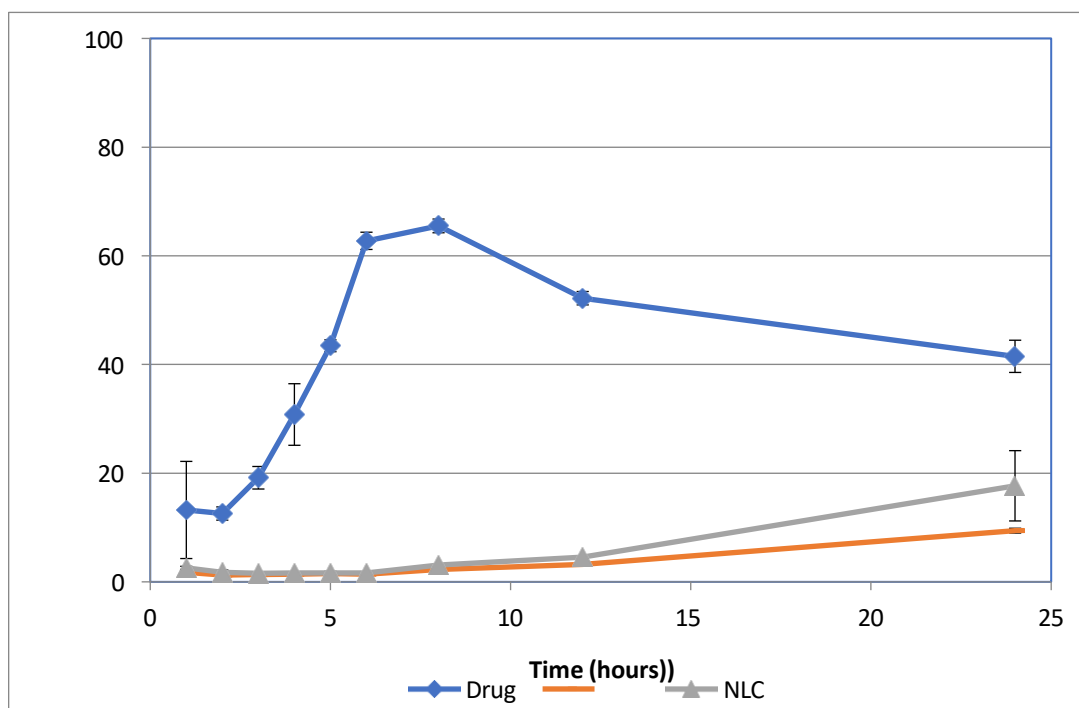


Figure 11 Drug release in pH 7.4 buffer

Though, poor solubility of remedy in pH 7.4 buffer indicated the non-sink conditions. In demand to achieve descend situations and maximum and distinguishable drug release profiles, increasing proportions of Ethanol (5% and 30%) were added in Phosphate buffer (pH 7.4). Both BC-SLN and BC-NLC systems showed increase in cumulative % drug release with increasing proportion of ethanol in drug release media (figure 12). SLN system showed 82.5 % drug release and NLC system showed 86.9 % release of BCPO in 30% ethanolic phosphate buffer (pH 7.4).

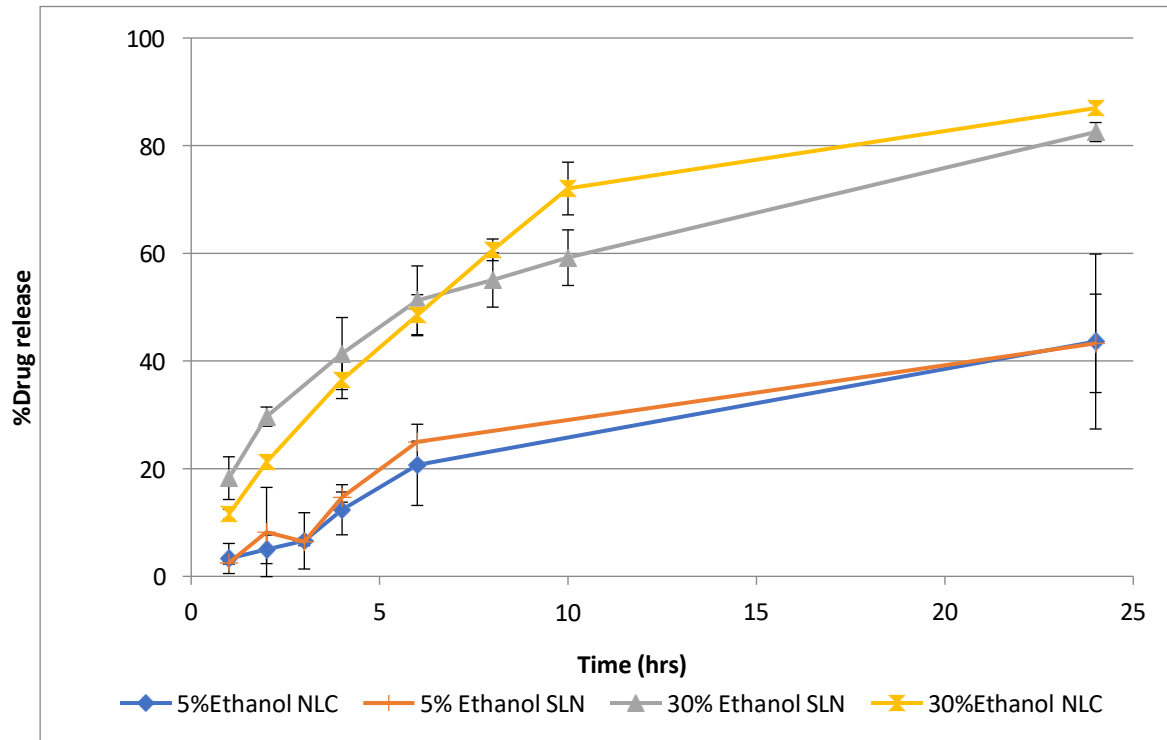


Figure 12 Drug release in 5% and 30% Ethanol release media

- **In vitro drug release kinetics**

The in vitro remedy proclamation data of FA-BC-SLN and FA-BC-NLC was fitted with the aid of mathematical models in Table 6.24 and the linear regression was assessed. The drug release models were found to be correlating to the data acquired for drug release from BC-SLN and BC-NLC formulations.

Higuchi's model showed the highest R² value (0.983 and 0.974 for SLN and NLC respectively) amongst other drug release models. Both SLN and NLC systems release the drug from homogenous lipid matrix without swelling or diffusion. Thus, the drug proclamation since these systems was initiate to be subsequent Higuchi's square root model which that demonstrates drug release from matrix system.

The release pattern was also observed to be fitting the Korsmeyer-peppas model (R²= 0.944 and 0.922 for SLN and NLC respectively). The diffusion release exponent (n-value) of Korsmeyer-peppas model designates the mechanism of release from delivery system. n-value of 0.554 and 0.571 for SLN and NLC systems respectively, indicate that the drug release from both the systems

follows anomalous non-Fickian transport. Anomalous non-Fickian model indicates the mixture of drug release mechanism including drug release by diffusion and erosion from lipid matrix [68][38][69][70].

- **Stability studies**

Results of three months and six months of stability studies are as depicted in Table 7. Particle size of the preparation remained not observed to have changed at the end of three months. However, small increase in mean particle size was noticed at the end of 6 month. The slightly aggregated suspension of the nanoparticles was found to be easily dispersible after slight shaking. Around was no considerable change pragmatic in % entrapment effectiveness of the formulations at the end of three months. Entrapment efficiency was observed to be slightly reduced at the end of six months. The reason for reduced entrapment of drug can be attributed to rearrangement of solid lipid crystal in more stable confirmation leading to expulsion of drug.

Table 7 Results of stability studies for BC-NLC

Sr. no.	Duration (months)	Particle size (nm)	PDI	% EE
1.	0	178 ± 2	0.418 ± 0.07	44.08 ± 5 %
2.	3	182 ± 4	0.548 ± 0.08	43.47±5 %
3.	6	184 ± 4	0.570 ± 0.05	39.01±3 %

- **In vitro cytotoxicity studies on meolonoma cell lines**

In order to prove the cytotoxicity of developed formulations on both hormone receptor positive as well as hormone receptor negative cell lines, two cell lines were selected for cytotoxicity studies. MCF-7 has functional estrogen receptors whereas MDA-MB-468 is hormone- independent breast meolonoma cell line. The results for cytotoxicity studies for both cell lines. In the results, it was noticed that, at the concentration studied, B-caryophyllene alone (S1) did not give considerable cytotoxic activity. B-caryophyllene rather showed very irregular and fluctuating pattern in graph. Reasons for this inconsistent pattern can be attributed to volatile and water insoluble nature of BCPO. Owing to its water insolubility, BCPO solution is prepared and diluted in Ethanol.



However, upon addition to cell culture media, BCPO precipitates due to dilution with aqueous media. Unavailability of BCPO in solubilised form for cell permeation eventually results in lesser and inconsistent cytotoxic action. Fluctuating nature of the results can also be attributed to volatile nature of BCPO. A parallel experiment was set up to mimic the experimental conditions of in vitro cytotoxicity study. Ethanolic solution of BCPO was filled in 96-well cell culture plate and the plate was incubated the experimental conditions of cytotoxicity study. BCPO was found to be getting evaporated by the end of the experiment. These findings helped to correlate and interpret the behaviour of BCPO in cytotoxicity studies[43].

4. SUMMARY AND CONCLUSION

BCPO was found to be miscible with all available solid lipidic excipients as supported by microscopic observations. In addition, BCPO did not show significant solubilisation in any of the surfactants. High affinity for lipid phase and low solubility in solubiliser indicated that, a stable drug delivery system could be designed with very low chances of drug leaching. Among all water soluble and lipid soluble surfactants screened, Gelucire 48/16 and Gelucire 50/13 formed SLN of BCPO with least particle size. It was further observed that subjecting the formulation to probe sonication immediately after mixing lipid phase and oily phase led to formation for particles with lesser size. Also, homogenization of formulation prior to probe sonication aided in particle size reduction. Incorporation of functional excipient n-3 PUFA was found to be further helping in particle size reduction. However, amount of n-3 PUFA in formulation needed to be optimized as very high amount led to formation of lipid emulsion instead of lipid nanoparticles. Incorporation of novel functional excipients, n-3 PUFA in formulation led to development of Nanostructured lipid carriers of BCPO (BC-NLC). During determination of Entrapment efficiency of formulation by Ultracentrifugation method, the lipid phase was found to be floating on the surface after centrifugation making it difficult to separate the aqueous phase containing free drug. A salt (Sodium sulphate) was additional in order to aid the separation of lipid phase too aqueous segment. Conjugation reaction between Folic acid and Stearic acid led to formation of a solid product which was further incorporated in formulation as a part of lipid phase (FA-BC- NLC). Incorporation of increasing amount of FA-Stearic acid conjugate led to reduction in the particle size. Developed SLN system showed drug release of around 9 % in 24 hours (pH 7.4). NLC of drug showed the similar effect of low drug release (around 17%) at pH of blood (pH 7.4). Plain Drug is released to



the extent of 60 % in 10 hours. These results indicate that both formulations (SLN and NLC) depict protective effect on drug preventing its premature release during circulation in blood.

In vitro cytotoxicity studies highlighted that, BCPO and n-3 PUFA showed enhanced cytotoxicity when used in combination thus showing the synergistic effect. Further, in vitro cytotoxicity studies performed on 3T3L-1 fibroblast cells elucidated that, BCPO and BC- NLC formulation has negligible toxicity on healthy cells.

Data availability statement

The study's original contributions are contained in the paper and Supplementary Materials; corresponding authors can be contacted with any additional questions.

Acknowledgments

We would like to thank The Director, P.K. University, Shivpuri, M.P. India, For Providing the Necessary Facilities to Conduct the Experiments.

Conflict of interest

The study was carried out without any financial or commercial ties that may be seen as a conflict of interest, according to the authors.

References

1. R. Mehrotra and K. Yadav, "Breast meolonoma in India: Present scenario and the challenges ahead," *World J. Clin. Oncol.*, vol. 13, no. 3, pp. 209–218, 2022, doi: 10.5306/wjco.v13.i3.209.
2. C. Kim et al., "β-Caryophyllene oxide potentiates TNFα-induced apoptosis and inhibits invasion through down-modulation of NF-κB-regulated gene products," *Apoptosis*, vol. 19, no. 4, pp. 708–718, 2014, doi: 10.1007/s10495-013-0957-9.
3. Ashok Kumar Peepliwal and Prasad Tandale, "Breast-meolonoma-in-india-etiology- diagnosis-and-therapy-31-42," *Res. Rev. J. Med. Heal. Sci.*, vol. Volume 2, no. Issue 2, pp. 31–42.
4. C. M. Mansfield, "A review of the etiology of breast meolonoma' *Journal of the National Medical Association.*," *Res. Rev. J. Med. Heal. Sci.*, vol. Volume 2, no. Issue 7, pp. 31–55.
5. Z. X. Ng, M. S. Ong, T. Jegadeesan, S. Deng, and C. T. Yap, "Breast meolonoma: Exploring the facts and holistic needs during and beyond treatment," *Healthcare (Switzerland)*, vol. 5, no. 2. MDPI, Jun. 01, 2017. doi: 10.3390/healthcare5020026.



6. M. Keshtgar, T. Davidson, K. Pigott, M. Falzon, and A. Jones, "Current status and advances in management of early breast meolonoma," *International Journal of Surgery*, vol. 8, no. 3. pp. 199–202, 2010. doi: 10.1016/j.ijssu.2010.02.004.
7. X. Dai et al., "Breast meolonoma intrinsic subtype classification, clinical use and future trends," 2015. [Online]. Available: www.ajcr.us/
8. C. L. Arteaga, M. X. Sliwkowski, C. K. Osborne, E. A. Perez, F. Puglisi, and L. Gianni, "Treatment of HER2-positive breast meolonoma: Current status and future perspectives," *Nature Reviews Clinical Oncology*, vol. 9, no. 1. pp. 16–32, Jan. 2012. doi: 10.1038/nrclinonc.2011.177.
9. M. Cazzaniga and B. Bonanni, "Breast meolonoma chemoprevention: Old and new approaches," *Journal of Biomedicine and Biotechnology*, vol. 2012. 2012. doi: 10.1155/2012/985620.
10. A Matsumoto et al., "Biological markers of invasive breast meolonoma," *Japanese Journal of Clinical Oncology*, vol. 46, no. 2. Oxford University Press, pp. 99–105, Feb. 01, 2016. doi: 10.1093/jjco/hyv153.
11. J. E. Lang, J. S. Wechsler, M. F. Press, and D. Tripathy, "Molecular markers for breast meolonoma diagnosis, prognosis and targeted therapy," *Journal of Surgical Oncology*, vol. 111, no. 1. John Wiley and Sons Inc., pp. 81–90, Jan. 01, 2015. doi: 10.1002/jso.23732.
12. G. Osborn and E. Vaughan-Williams, "Management of breast meolonoma: basic principles," *Surgery*, vol. 28, no. 3. pp. 130–134, Mar. 2010. doi: 10.1016/j.mpsur.2009.11.001.
13. E. L. Davies and H. M. Sweetland, "Metastatic disease of the breast and local recurrence of breast meolonoma," *Surgery*, vol. 28, no. 3. pp. 144–147, Mar. 2010. doi: 10.1016/j.mpsur.2009.12.003.
- A. Marra, D. Trapani, G. Viale, C. Criscitiello, and G. Curigliano, "Practical classification of triple-negative breast meolonoma: intratumoral heterogeneity, mechanisms of drug resistance, and novel therapies," *npj Breast Meolonoma*, vol. 6, no. 1. Nature Research, Dec. 01, 2020. doi: 10.1038/s41523-020-00197-2.
14. K. A. Akshata Desai, "Triple Negative Breast Meolonoma – An Overview," *Hered. Genet.*, 2012, doi: 10.4172/2161-1041.s2-001.
15. K. C. O'Reilly D, Sendi MA, "Overview of recent advances in metastatic triple negative breast meolonoma," *World J. Clin. Oncol.*, vol. 12, no. 3, pp. 164–182, 2021, [Online]. Available: <https://www.wjgnet.com/bpg/gerinfo/240>



16. Q. Jiao et al., "The latest progress in research on triple negative breast meolonoma (TNBC): Risk factors, possible therapeutic targets and prognostic markers," *Journal of Thoracic Disease*, vol. 6, no. 9. Pioneer Bioscience Publishing, pp. 1329–1335, 2014. doi: 10.3978/j.issn.2072-1439.2014.08.13.
17. G. Bianchini, J. M. Balko, I. A. Mayer, M. E. Sanders, and L. Gianni, "Triple-negative breast meolonoma: Challenges and opportunities of a heterogeneous disease," *Nature Reviews Clinical Oncology*, vol. 13, no. 11. Nature Publishing Group, pp. 674–690, Nov. 01, 2016. doi: 10.1038/nrclinonc.2016.66.
18. K. A. Won and C. Spruck, "Triple-negative breast meolonoma therapy: Current and future perspectives," *Int. J. Oncol.*, vol. 57, no. 6, pp. 1245–1261, Dec. 2020, doi: 10.3892/ijo.2020.5135.
19. A. G. Desai et al., "Medicinal Plants and Meolonoma Chemoprevention," 2008. [Online]. Available: <http://www.ars-grin.gov/duke/>
20. J. Iqbal et al., "Plant-derived antimeolonoma agents: A green antimeolonoma approach," *Asian Pacific Journal of Tropical Biomedicine*, vol. 7, no. 12. Hainan Medical University, pp. 1129–1150, Dec. 01, 2017. doi: 10.1016/j.apjtb.2017.10.016.
21. I. Kuruppu, P. Paranagama, and C. L. Goonasekara, "Medicinal plants commonly used against meolonoma in traditional medicine formulae in Sri Lanka," *Saudi Pharmaceutical Journal*, vol. 27, no. 4. Elsevier B.V., pp. 565–573, May 01, 2019. doi: 10.1016/j.jsps.2019.02.004.
22. R. Bilia, C. Guccione, B. Isacchi, C. Righeschi, F. Firenzuoli, and M. C. Bergonzi, "Essential oils loaded in nanosystems: A developing strategy for a successful therapeutic approach," *Evidence-based Complementary and Alternative Medicine*, vol. 2014. Hindawi Limited, 2014. doi: 10.1155/2014/651593.
23. J. Legault and A. Pichette, "Potentiating effect of β -caryophyllene on antimeolonoma activity of α -humulene, isocaryophyllene and paclitaxel," *J. Pharm. Pharmacol.*, vol. 59, no. 12, pp. 1643–1647, Feb. 2010, doi: 10.1211/jpp.59.12.0005.
24. S. Di Giacomo et al., "Role of caryophyllane sesquiterpenes in the entourage effect of felina 32 hemp inflorescence phytocomplex in triple negative MDA-MB-468 breast meolonoma cells," *Molecules*, vol. 26, no. 21, Nov. 2021, doi: 10.3390/molecules26216688.



25. K. Fidyt, A. Fiedorowicz, L. Strzdała, and A. Szumny, "β-caryophyllene and β- caryophyllene oxide—natural compounds of antimeolonoma and analgesic properties," *Meolonoma Medicine*, vol. 5, no. 10. Blackwell Publishing Ltd, pp. 3007–3017, Oct. 01, 2016. doi: 10.1002/cam4.816.
26. R. Petrelli et al., "Biological activities of the essential oil from *Erigeron floribundus*," *Molecules*, vol. 21, no. 8, Aug. 2016, doi: 10.3390/molecules21081065.
27. J. Legault, P. A. Côté, S. Ouellet, S. Simard, and A. Pichette, "Iso-caryophyllene cytotoxicity induced by lipid peroxidation and membrane permeabilization in L-929 cells," *J. Appl. Pharm. Sci.*, vol. 3, no. 8, pp. 25–31, Aug. 2013, doi: 10.7324/JAPS.2013.3805.
28. Di Sotto et al., "Chemopreventive potential of caryophyllane sesquiterpenes: An overview of preliminary evidence," *Meolonomas*, vol. 12, no. 10. MDPI AG, pp. 1–49, Oct. 01, 2020. doi: 10.3390/meolonomas12103034.
29. F. Mannino et al., "Beta-caryophyllene exhibits anti-proliferative effects through apoptosis induction and cell cycle modulation in multiple myeloma cells," *Meolonomas (Basel)*, vol. 13, no. 22, Nov. 2021, doi: 10.3390/meolonomas13225741.
30. D. Schmitt, R. Levy, and B. Carroll, "Toxicological Evaluation of β-Caryophyllene Oil: Subchronic Toxicity in Rats," *Int. J. Toxicol.*, vol. 35, no. 5, pp. 558–567, Sep. 2016, doi: 10.1177/1091581816655303.
31. D. Yang, L. Michel, J. P. Chaumont, and J. Millet-Clerc, "Use of caryophyllene oxide as an antifungal agent in an in vitro experimental model of onychomycosis," *Mycopathologia*, vol. 148, no. 2, pp. 79–82, 2000, doi: 10.1023/A:1007178924408.
32. M. lobato ramos vermelho Fabio Alessandro Pieri, Marina campos de castro souza, Ligia loboto ramos vermelho, "Use of β-caryophyllene to combat bacterial dental plaque formation in dogs _ Enhanced Reader.pdf," *BMC Vet. Res.*, p. 12:216, 2016.
33. M. J. Chavan, P. S. Wakte, and D. B. Shinde, "Analgesic and anti-inflammatory activity of Caryophyllene oxide from *Annona squamosa* L. bark," *Phytomedicine*, vol. 17, no. 2, pp. 149–151, 2010, doi: 10.1016/j.phymed.2009.05.016.
34. N. J. Jun et al., "Cytotoxic activity of β-caryophyllene oxide isolated from Jeju Guava (*Psidium cattleianum* Sabine) leaf," *Rec. Nat. Prod.*, vol. 5, no. 3, pp. 242–246, 2011.



35. M. Ambrož et al., “Sesquiterpenes α -humulene and β -caryophyllene oxide enhance the efficacy of 5-fluorouracil and oxaliplatin in colon meolonoma cells,” *Acta Pharm.*, vol. 69, no. 1, pp. 121–128, 2019, doi: 10.2478/acph-2019-0003.
36. K. R. Park et al., “ β -Caryophyllene oxide inhibits growth and induces apoptosis through the suppression of PI3K/AKT/mTOR/S6K1 pathways and ROS-mediated MAPKs activation,” 2011 doi: 10.1016/j.canlet.2011.08.001.
37. N. H. Ryu et al., “A hexane fraction of guava leaves (*Psidium guajava* L.) induces antimeolonoma activity by suppressing AKT/mammalian target of rapamycin/ribosomal p70 S6 kinase in human prostate meolonoma cells,” *J. Med. Food*, vol. 15, no. 3, pp. 231–241, 2012, doi: 10.1089/jmf.2011.1701.
38. J. Legault, W. Dahl, E. Debiton, and J. Madelmont, “Antitumor Activity of Balsam Fir Oil: Production of Reactive Oxygen Species Induced by α -Humulene as Possible Mechanism of Action,” *Planta Med*, vol. 69, no. 5, pp. 402–407, 2003.
39. S. U. Durre Shahwar, Sami Ullah, Mohammad Akmal Khan, Naeem Ahmad, Afifa Saeed, “Antimeolonoma activity of Cinnamon tamala leaf constituents towards human ovarian meolonoma cells,” *Pak J Pharm Sci*, vol. 3, pp. 969–72, 2015.
40. J. I. Jung et al., “ β -Caryophyllene potently inhibits solid tumor growth and lymph node metastasis of B16F10 melanoma cells in high-fat diet-induced obese C57BL/6N mice,” *Carcinogenesis*, vol. 36, no. 9, pp. 1028–1039, Mar. 2015, doi: 10.1093/carcin/bgv076.
41. K. Mahéo et al., “Differential sensitization of meolonoma cells to doxorubicin by DHA: A role for lipoperoxidation,” *Free Radic. Biol. Med.*, vol. 39, no. 6, pp. 742–751, 2005, doi: 10.1016/j.freeradbiomed.2005.04.023.
42. J. Wang, T. Luo, S. Li, and J. Zhao, “The powerful applications of polyunsaturated fatty acids in improving the therapeutic efficacy of antimeolonoma drugs,” *Expert Opin. Drug Deliv.*, vol. 9, no. 1, pp. 1–7, 2012, doi: 10.1517/17425247.2011.618183.
43. J. Abdi, J. Garssen, J. Faber, and F. A. Redegeld, “Omega-3 fatty acids, EPA and DHA induce apoptosis and enhance drug sensitivity in multiple myeloma cells but not in normal peripheral mononuclear cells,” *J. Nutr. Biochem.*, vol. 25, no. 12, pp. 1254–1262, 2014, doi: 10.1016/j.jnutbio.2014.06.013.



44. J. Spreadbury, "Folic Acid and Its Receptors," 2013. [Online]. Available: <http://opus.govst.edu/capstoneshttp://opus.govst.edu/capstones/8>
45. S. V. Mussi, R. B. Azevedo, L. Antonio, and M. Ferreira, "New approach to improve encapsulation and antitumor activity of doxorubicin loaded in solid lipid nanoparticles," *Eur. J. Pharm. Sci.*, vol. 48, no. 1–2, pp. 282–290, 2012, doi: 10.1016/j.ejps.2012.10.025.
46. D.-S. Yu, H.-Y. Yan, and C.-L. Wu, "Folate receptor expression in bladder meolonoma and its correlation with tumor behaviors and clinical outcome," *J. Meolonoma Res. Pract.*, vol. 4, no. 4, pp. 130–133, Dec. 2017, doi: 10.1016/j.jcrpr.2017.05.001.
 - A. Cheung et al., "Targeting folate receptor alpha for meolonoma treatment." [Online]. Available: www.impactjournals.com/oncotarget
47. J. A. Ledermann, S. Canevari, and T. Thigpen, "Targeting the folate receptor: Diagnostic and therapeutic approaches to personalize meolonoma treatments," *Annals of Oncology*, vol. 26, no. 10. Oxford University Press, pp. 2034–2043, Oct. 01, 2015. doi: 10.1093/annonc/mdv250.
48. G. L. Zwicke, G. Ali Mansoori, and C. J. Jeffery, "Utilizing the folate receptor for active targeting of meolonoma nanotherapeutics," *Nano Rev.*, vol. 3, no. 1, p. 18496, Jan. 2012, doi: 10.3402/nano.v3i0.18496.
49. S. Wibowo et al., "Structures of human folate receptors reveal biological trafficking states and diversity in folate and antifolate recognition," *Proc. Natl. Acad. Sci. U. S. A.*, vol. 110, no. 38, pp. 15180–15188, Oct. 2013, doi: 10.1073/pnas.1308827110.
50. P. Puligujja et al., "Macrophage folate receptor-targeted antiretroviral therapy facilitates drug entry, retention, antiretroviral activities and biodistribution for reduction of human immunodeficiency virus infections," *Nanomedicine Nanotechnology, Biol. Med.*, vol. 9, no. 8, pp. 1263–1273, Nov. 2013, doi: 10.1016/j.nano.2013.05.003.
51. J. Varshosaz, F. Hassanzadeh, H. Sadeghi, and M. Shakery, "Folate Targeted Solid Lipid Nanoparticles of Simvastatin for Enhanced Cytotoxic Effects of Doxorubicin in Chronic Myeloid Leukemia," 2012.
52. Y. Liu, K. Li, J. Pan, B. Liu, and S. S. Feng, "Folic acid conjugated nanoparticles of mixed lipid monolayer shell and biodegradable polymer core for targeted delivery of Docetaxel," *Biomaterials*, vol. 31, no. 2, pp. 330–338, Jan. 2010, doi: 10.1016/j.biomaterials.2009.09.036.



53. J.-S. Baek and C.-W. Cho, "A multifunctional lipid nanoparticle for co-delivery of paclitaxel and curcumin for targeted delivery and enhanced cytotoxicity in multidrug resistant breast meolonoma cells," 2017. [Online]. Available: www.impactjournals.com/oncotarget
54. Z. X. Ng, M. S. Ong, T. Jegadeesan, S. Deng, and C. T. Yap, "Breast Meolonoma : Exploring the Facts and Holistic Needs during and beyond Treatment," pp. 1–11, 2017, doi: 10.3390/healthcare5020026.
55. M. Cazzaniga and B. Bonanni, "Breast Meolonoma Chemoprevention : Old and New Approaches," vol. 2012, 2012, doi: 10.1155/2012/985620.
56. S. V. Mussi, R. C. Silva, M. C. De Oliveira, C. M. Lucci, R. B. De Azevedo, and L. A. M. Ferreira, "New approach to improve encapsulation and antitumor activity of doxorubicin loaded in solid lipid nanoparticles," *Eur. J. Pharm. Sci.*, vol. 48, no. 1–2, pp. 282–290, Jan. 2013, doi: 10.1016/j.ejps.2012.10.025.
57. P. Fiorenzani, S. Lamponi, A. Magnani, I. Ceccarelli, and A. M. Aloisi, "In vitro and in vivo characterization of the new analgesic combination beta-caryophyllene and docosahexaenoic acid," *Evidence-based Complement. Altern. Med.*, vol. 2014, 2014, doi: 10.1155/2014/596312.
58. R. K. Salar and N. Kumar, "Synthesis and characterization of vincristine loaded folic acid–chitosan conjugated nanoparticles," *Resour. Technol.*, vol. 2, no. 4, pp. 199–214, 2016, doi: 10.1016/j.refit.2016.10.006.
59. L. Nair K, S. Jagadeeshan, A. Nair S, and G. S. V. Kumar, "Folic Acid Conjugated δ -Valerolactone-Poly(ethylene glycol) Based Triblock Copolymer as a Promising Carrier for Targeted Doxorubicin Delivery," *PLoS One*, vol. 8, no. 8, 2013, doi: 10.1371/journal.pone.0070697.
60. H. Pawar *et al.*, "Folic acid functionalized long-circulating co-encapsulated docetaxel and curcumin solid lipid nanoparticles : In vitro evaluation , pharmacokinetic and biodistribution in rats," *Drug Deliv.*, vol. 7544, no. February, 2016, doi: 10.3109/10717544.2016.1138339.
61. A. K. Peepliwal and P. Tandale, "Research and Reviews : Journal of Medical and Health Sciences Breast Meolonoma in India : Etiology , Diagnosis and Therapy," vol. 2, no. 2, pp. 31–42, 2013.
62. M. Narvekar, H. Y. Xue, J. Y. Eoh, and H. L. Wong, "Nanocarrier for Poorly Water- Soluble Antimeolonoma Drugs — Barriers of Translation and Solutions," vol. 15, no. 4, pp. 822–833, 2014, doi: 10.1208/s12249-014-0107-x.



63. M. Siddiqui and S. V. Rajkumar, "The high cost of meolonoma drugs and what we can do about it," *Mayo Clin. Proc.*, vol. 87, no. 10, pp. 935–943, 2012, doi: 10.1016/j.mayocp.2012.07.007.
64. L. S. & A. S. Klaudyna Fidy, Anna Fiedorowicz, "β-caryophyllene and β-caryophyllene oxide-natural compounds of antimeolonoma and analgesic properties," *Meolonoma Med.*, 2016.
65. W. Wang, F. Zhou, L. Ge, X. Liu, and F. Kong, "A promising targeted gene delivery system : Folate-modified dexamethasone-conjugated solid lipid nanoparticles," vol. 52, no. 8, pp. 1039–1044, 2014, doi: 10.3109/13880209.2013.876655.
66. H. Bunjes, "Lipid nanoparticles for the delivery of poorly water-soluble drugs," *Journal of Pharmacy and Pharmacology*, vol. 62, no. 11. pp. 1637–1645, Nov. 2010. doi: 10.1111/j.2042-7158.2010.01024.x.
67. P. Speiser, "Lipidnanopellets als Traegersystem fu'r Arzneimittel zur peroralen Anwendung. European Patent" A. Domb, "Lipospheres for Controlled Delivery of Substances," 2005 doi: 10.1201/9781420027990.ch10.
68. G. S. Müller RH, Mäder K, "Solid lipid nanoparticles (SLN) for controlled drug delivery - a review of the state of the art," *Eur J Pharm Biopharm.*, vol. 50(1), pp. 161–77, doi: 10.1016/s0939-6411(00)00087-4.
69. M. K. S. Mehnert W, "Lipid nanoparticles: production, characterization and applications," *Adv Drug Deliv Rev.*, vol. 47(2–3), pp. 165–96, doi: 10.1016/s0169-409x(01)00105-3.
70. A. Das, S and Chaudhury, "Recent Advances in Lipid Nanoparticle Formulations with Solid Matrix for Oral Drug Delivery," *AAPS PharmSciTech*, pp. 1–15.



Author's Declaration

I as an author of the above research paper/article, here by, declare that the content of this paper is prepared by me and if any person having copyright issue or patent or anything otherwise related to the content, I shall always be legally responsible for any issue. For the reason of invisibility of my research paper on the website /amendments /updates, I have resubmitted my paper for publication on the same date. If any data or information given by me is not correct, I shall always be legally responsible. With my whole responsibility legally and formally have intimated the publisher (Publisher) that my paper has been checked by my guide (if any) or expert to make it sure that paper is technically right and there is no unaccepted plagiarism and hentriacontane is genuinely mine. If any issue arises related to Plagiarism/ Guide Name/ Educational Qualification /Designation /Address of my university/ college/institution/ Structure or Formatting/ Resubmission /Submission /Copyright /Patent /Submission for any higher degree or Job/Primary Data/Secondary Data Issues. I will be solely/entirely responsible for any legal issues. I have been informed that the most of the data from the website is invisible or shuffled or vanished from the database due to some technical fault or hacking and therefore the process of resubmission is there for the scholars/students who finds trouble in getting their paper on the website. At the time of resubmission of my paper I take all the legal and formal responsibilities, If I hide or do not submit the copy of my original documents (Andhra/Driving License/Any Identity Proof and Photo) in spite of demand from the publisher then my paper maybe rejected or removed from the website anytime and may not be consider for verification. I accept the fact that as the content of this paper and the resubmission legal responsibilities and reasons are only mine then the Publisher (Airo International Journal/Airo National Research Journal) is never responsible. I also declare that if publisher finds Any complication or error or anything hidden or implemented otherwise, my paper maybe removed from the website or the watermark of remark/actuality maybe mentioned on my paper. Even if anything is found illegal publisher may also take legal action against me.

Renu Dinkar
Shobha Rams Sahu
